Korean J. Chem. Eng., 39(12), 3399-3411 (2022)
DOI: 10.1007/s11814-022-1239-4

pISSN: 0256-1115
eISSN: 1975-7220

Reactive extraction evaluation for vanadium (V) removal in the MRDC column using axial dispersion and central composition approach

Benyamin Shakib*, Mehdi Asadollahzadeh,†, Mohamamd Outokesh*, Rezvan Torkaman**, and Meisam Torab-Mostaedi****

*Department of Energy Engineering, Sharif University of Technology, P. O. Box 11365-8639, Tehran, Iran
**Nuclear Fuel Cycle Research School, Nuclear Science and Technology Research Institute, P. O. Box: 11365-8486, Tehran, Iran
(*Received 8 June 2021 • Revised 4 June 2022 • Accepted 19 July 2022*)

Abstract−Reactive extraction development was investigated to extract vanadium ions from sulfate solution in the modified rotating disc column (MRDC). It was found from batch experiments that D_2EHPA and TBP concentrations, initial aqueous phase pH, and the concentration of NH_4OH as a stripping agent were optimized equal to 0.3 M, 0.36 M, 2, and 1 M, respectively. In the continuous experiments, the effects of rotor speed, aqueous and organic phase flow rates, and mass transfer direction were investigated on the dispersed phase holdup, mass transfer coefficients, and vanadium extraction. The experiment design was based on the response surface design to analyze the dependence of responses with the input parameters. The uncertainty analysis by the Monte Carlo simulation indicates that the rotor speed, reaction conditions, and phase flow rates affected the dispersed phase holdup. By applying the axial dispersion model, the performance of mass transfer coefficients in terms of agitation speed, aqueous phase flow rate, organic phase flow rate, and mass transfer direction was evaluated under the chemical reaction system. A new model by considering the dimensionless numbers has been provided to predict overall mass transfer data based on the dispersed phase.

Keywords: Modified Rotating Disc Column (MRDC), Vanadium (V) Extraction, Axial Dispersion Model, Central Composition Approach, Monte Carlo Simulation

INTRODUCTION

The demand for heavy metals due to their significant enhancing usages has been increased in recent decades. High melting point and chemical resistance against corrosion for the vanadium element improve the extraction and separation techniques from minerals including vanadinite, roscoelite, and carnotite [1]. Recently, researchers have been studying separation methods for recovering the vanadium from various resources, such as oil flies, spent catalysts, seawater, and stone coal [2]. It is certified that solvent extraction is an important part of the separation process due to its importance in separating the heavy metals.

Numerous studies have been published for investigating the impact of diverse solvents such as 5,8-diethyl-7-hydroxyldodecane-6-oxime (LIX63) [3,4], 2-ethylexyl hydrogen 2-ethylhexyl phosphonate (PC 88A) [5,6], bis-2,4,4-trimethylpentyl phosphinic acid (Cyanex272) [7,8], trihexyl(tetradecyl)phosphonium chloride (Cyphos IL 101) [9,10], Di-(2-ethylhexyl)phosphoric acid (D2EHPA) [11, 12], and a mixture of trialkyl phosphine oxides (93%), with n-octyl and n-hexyl chains (Cyanex923) [13,14] on the separation and purification of vanadium from acidic and alkaline solutions. The addition of tributyl phosphate (TBP) extractant into the organic phase as a phase modifier and synergism effect is intended for reaching further extraction efficiency and avoid the emulsion formation for the separation of elements such as zirconium, zinc, cobalt, nickel, and molybdenum.

Agitated columns are broadly utilized in chemical and hydrometallurgical industries [15-17]. The rotating disc column (RDC) is one kind of mass transfer device in which embraces a number of sections shaped by an arrangement of stator rings, with a rotation disc centered in each step and upheld via the single turning shaft. Many studies have been performed on the RDC column's hydrodynamic parameters and mass transfer characteristics. However, the undesirable impacts due to its structure lead to a decline in the RDC column performance by considering inappropriate drop distribution and high axial mixing [18,19]. For these reasons, upgraded compartments of the RDC column, such as open turbine rotating disc contactor [20,21], asymmetric rotating disc contactor [22-24], and perforated rotating disc contactor [25-27] are also extended. The modified RDC column with the perforated structures leads to appropriate mass transfer performance due to an increase in the liquid-liquid dispersion [28-30].

The equipment design of the columns for chemical processes is far from consent by considering the reactive systems. The precise expectations of mass transfer evaluation optimize the design of the solvent extraction columns. The hydrodynamic characteristics, droplet behavior, interface versatility, slip velocity of drops, chemical resistance to mass transfer, and physical properties affect the mass transfer coefficients [31-35]. In previous studies, several investigators have studied the reactive systems for solvent extraction of metals such as cobalt, gadolinium, lanthanum, tellurium, and cerium in the pulsed

†To whom correspondence should be addressed.
E-mail: masadollahzadeh@aeoi.org.ir, mehdiasadollahzadeh@iust.ac.ir, mehdiasadollahzadeh@yahoo.com

or rotation columns. At present, limited information has been reported to evaluate the mass transfer data of the modified rotating disc column (MRDC) under reactive extraction conditions. Therefore, the novelty of this study is the extraction of vanadium ions by using a new extractor column (MRDC). Also, the direct extraction of vanadium from sulfate solution by a mixture of D_2EHPA and TBP was studied to evaluate the dispersed phase holdup and mass transfer data by the coupling effects of the central composition approach and Monte Carlo simulation in the MRDC column. The effect of operating variables, reaction conditions, physical properties, geometric term, and mass transfer direction on the holdup of the dispersed phase in the mentioned column was investigated. The feasibility of the axial dispersion model was examined with equations to predict the reactive mass transfer, and the applicability of available models to this column was reviewed. Eventually, a novel model is suggested to determine the dispersed phase mass transfer coefficients by considering the chemical resistance to mass transfer in the MRDC column.

AVAILABLE MATHEMATICAL MODELS

The outer coefficient is required for chemical reaction systems in which ions are exchanged between the interface of dispersed phase droplets and the bulk aqueous phase to determine the overall mass transfer data. Forced or normal convection, as well as molecular dissemination, are generally classified for modeling the dispersed phase mass transfer performance. The different semi-empirical and theoretical models to calculate the mass transfer data are described in the available literature based on the droplet movement into or out of droplets in the aqueous phase. Gröber proposed the following equation to investigate the mass transfer coefficients by considering the atomic diffusivity within the rigid spherical droplets [36]:

$$K_{od}=-\left(\frac{d}{6t}\right)\ln\left[6\sum_{n=1}^{\infty}B_n\exp\left(-\frac{4\lambda_n^2 D_d t}{d^2}\right)\right] \quad (1)$$

The negligibility of external resistance to mass transfer and lower values than units for Reynold number leads to calculating the circulation motions inside of drops with the relative velocity of droplets in the aqueous phase. By considering the laminar condition, the internal streamlines of the droplets can be obtained by this equation. The output result for the laminar internal circulation owing to smaller drop size is given by Kronig and Brink as below [37]:

$$K_{od}=-\left(\frac{d}{6t}\right)\ln\left[\left(\frac{3}{8}\right)\sum_{n=1}^{\infty}B_n^2\exp\left(-\frac{64\lambda_n D_d t}{d^2}\right)\right] \quad (2)$$

Handlos and Baron proposed the following relation based on internal circulation patterns, which is utilized for resistance in both phases at higher Reynolds number [38]:

$$K_{od}=-\left(\frac{d}{6t}\right)\ln\left[6\sum_{n=1}^{\infty}B_n^2\exp\left(-\frac{\lambda_n V_t t}{128d^2(1+k)}\right)\right] \quad (3)$$

Table 1. Published models for calculating the enhancement factor in different mass transfer devices

Equation		Comment	Investigator
$R=0.003\left(\rho_c\frac{dV_t}{\mu_c}\right)^2\left(\frac{1}{1+k}\right)^2$	(5)	Single drop system	Boyadzhiev et al. [48]
$R=1+0.177Re^{0.43}Sc_d^{0.23}\left(\frac{1}{1+k}\right)^{0.89}$	(6)	Single drop system	Steiner [49]
$R=0.243+0.785Re^{0.85}(1-\varphi)^{7.07}$	(7)	Kühni column	Hemmati at al. [50]
$R=-0.34+0.15Re^{1.03}(1-\varphi)Eö^{-0.33}$	(8)	Oldshue Rushton column	Asadollazadeh et al. [51]
$D_{eff}=4.5151\times10^{-9}\exp(0.0067Re)$	(9)	Pulsed perforated plate column	Bahmanyar et al. [52]
$R=-13.33+36.69Re^{-0.135}(1-\varphi)Eö^{0.16}$ (c→d) $R=-11.86+63.38Re^{-0.237}(1-\varphi)Eö^{0.3}$ (d→c)	(10)	Pulsed disc and doughnut column	Torab-Mostaedi et al. [53]
$R=5.56\times10^{-5}\left(\frac{2Re}{1+k}\right)^{1.42}\left(\frac{g\Delta\rho d_{32}^2}{\sigma}\right)^{0.12}Sc_d^{0.67}(1-\varphi)$	(11)	Spray column	Steiner et al. [54]
$R=0.0272(1+h^{-1})Re^{1.258}$	(12)	Regular packed column	Rahbar-Kelishami et al. [55]
$R=-1.69+2.912Re^{0.12}(1-\varphi)Eö^{0.058}$	(13)	Oldshue Rushton column	Shakib et al. [56]
$R=-0.79+0.48Re^{0.67}$	(14)	Asymmetric rotating disc contactor column	Torab-Mostaedi et al. [57]
$R=-14.9+41.1Re^{-0.158}(1-\varphi)^{-0.95}Eö^{0.31}$ (c→d) $R=-11.68+34.67Re^{-0.161}(1-\varphi)^{-0.95}Eö^{0.21}$ (d→c)	(15)	Pulsed disc and doughnut column	Torkaman et al. [58]
$D_{eff}=0.4755\times10^{-9}Re^{0.65}$	(16)	Rotating disc contactor column	Amanabadi et al. [59]
$R=-0.51+1.74Re^{0.313}(1-\varphi)Eö^{0.165}$	(17)	Perforated rotating disc contactor column	Hemmati et al. [60]
$R=0.51+2.13Re^{-0.257}(1-\varphi)Eö^{14.2}$	(18)	Hanson mixer-settler column	Torab-Mostaedi et al. [61]
$R=-2.57+1326.07Re^{0.50}(1+k)^{-0.8}Sc_C^{-0.94}$	(19)	Pulsed packed column	Torab-Mostaedi and Safdari [62]

The oscillating motion in the solvent phase drops happens by enhancing the flow patterns in which the development of comprehensive relation for determining the mass transfer data inside oscillating drops was expanded. The effective diffusivity instead of molecular diffusivity was recommended to remove the errors of the previous equations in order to develop the equation for mass transfer evaluation. The calculation of mass transfer performance in the solvent extraction column based on the extensive range of drop distribution is unreliable based on the variations in the transfer mechanisms inside dispersed phase droplets. The mentioned equation to calculate the dispersed phase mass transfer of dispersed phase was proposed by Johnson and Hamielec as follows [39]:

$$K_{od}=-\left(\frac{d}{6t}\right)\ln\left[6\sum_{n=1}^{\infty}B_n\exp\left(-\frac{4\lambda_n^2RD_dt}{d^2}\right)\right] \quad (4)$$

Several authors have published variant equations for calculating the enhancement factor by applying the effective diffusivity in various mass transfer devices. It is found that applying this enhancement factor plays a critical role in determining the values of mass transfer data. The published models for obtaining the overall mass transfer coefficients of the dispersed phase in different agitated and pulsed columns are presented in Table 1. Also, the mass transfer coefficient of the dispersed phase for different extraction columns was proposed by Kumar and Hartland that the semi-empirical equation for RDC column represented as below [40]:

$$\frac{\frac{Sh_c}{(1-\varphi)}-Sh_{C,\,rigid}}{Sh_{C,\,\infty}-\frac{Sh_c}{(1-\varphi)}}=0.0526Re^{1/3+0.0659Re^{0.025}}SC_C^{1/3}\left(\frac{V_S\mu_C}{\sigma}\right)^{1/3}\frac{1}{1+k^{1.1}} \quad (20)$$

$$Sh_{C,\,rigid}=2.43+0.775Re^{1/2}SC_C^{1/3}+0.0103ReSC_C^{1/3} \quad (21)$$

$$Sh_{C,\,\infty}=50+\frac{2}{\sqrt{\pi}}Pe_C^{1/2} \quad (22)$$

$$Sh_d=17.7+\frac{0.00319(ReSC_d^{1/3})^{1.7}}{1+0.0143(ReSC_d^{1/3})^{0.7}}\left(\frac{\rho_d}{\rho_c}\right)^{2/3}\frac{1}{1+k^{2/3}} \quad (23)$$

$$\frac{1}{K_{od}}=\frac{m}{k_c}+\frac{1}{k_d} \quad (24)$$

EXPERIMENTAL

Herein, the solvent extraction experiments were conducted in batch and continuous mode. The achievement of the batch study is for the optimization of the operating variables for vanadium separation from sulfate solution by synergistic effects of D_2EHPA and TBP for obtaining the maximum efficiency. Then, the feasibility of the modified RDC column in the field of heavy metal extraction was studied. The effect of the operational variables, hydrodynamic parameters, and mass transfer direction was investigated on the mass transfer data under the chemical reaction system.

1. Materials

The used extractants were D_2EHPA and TBP produced by Sigma-Aldrich and Merck companies, respectively, which were mixed in kerosene supplied in the Tehran refinery for preparing the needed concentration. The synthetic aqueous solution was obtained by dissolving 200 mg/L of generated $NaVO_3$ by Sigma-Aldrich Company in distilled water. Sulfuric acid (Merck, 98%), and sodium hydroxide (Sigma-Aldrich, 97%) were used as the initial pH adjuster of the aqueous phase.

2. Apparatus

The collected samples of the aqueous phase were analyzed for determining the vanadium concentration by a UV/Vis spectrophotometer (UNICO model). The vanadium concentration of the organic phase was calculated by the mass balance approach. The experiments in order to mix the aqueous and organic phases were carried out by a mechanical shaker (CH-4103Bottmingen). The acidity of aqueous phase was measured with the digital pH meter (Sartorius PB-11 model) for analytical purposes.

3. Physical Properties

In this study, densities of the continuous and the dispersed phases were calculated by the pycnometer methodology. The viscosities of both fluids were also determined via DVI-Prime viscometer. The interfacial tension in extraction and stripping stages was obtained with a Krüss tensiometer. Wilke and Chang equation was applied to calculate the vanadium diffusivity coefficients in the aqueous and organic phases [41]. The mean concentrations of vanadium ions in both different immiscible fluids at the inlet and outlet of the extractor were obtained to eliminate the measurement errors of interfacial tension due to the uncertainty in physical properties.

4. Batch Experiments Method

Extraction and stripping tests were carried out in a 100 cc screw cap bottle using a mechanical shaker for 30 min. Equal volumes of aqueous and organic phases (10 mL) were introduced into the container and thoroughly mixed. After mixing, the solution was decanted into a separator funnel for phase separation. Vanadium content in the organic phase and aqueous phase was obtained by applying a mass balance and UV spectrometry, respectively. The extraction and stripping percentages in the equal volumes and the synergistic enhancement factor based on the synergism theory are defined as follows:

$$E\%=\frac{[M]_{org}}{[M]_{org}+[M]_{aq}}\times 100 \quad (25)$$

$$S\%=\frac{[M]_{aq,\,s}}{[M]_{org}+[M]_{aq,\,s}}\times 100 \quad (26)$$

$$SEF=\frac{D_{mix}}{D_{D2EHPA}+D_{TBP}} \quad (27)$$

5. Continuous Experiments Method

The solvent extraction experiments were performed in the MRDC column with perforated structures; this equipment was constructed by the internal diameter and active height equal to 113 mm and 1,430 mm, respectively. Mixing of fluids was accomplished by the discs of 70 mm diameter located at the center of the column, and these discs were moved by an electric stimulant by applying the variable gearbox. The column length consisted of 43 stages. This extractor is equipped with two pumps and flow meters to pump the fluids and measure the flow rates. The discs, stator rings, and both settling sections were made of stainless steel. The distribution of the aqueous and organic phases was placed at the top and bottom of the column, respectively. Torab-Mostaedi et al. previously

described that the changes in the interface are controlled considering the optical sensor in the specific area of the solvent extraction column [42]. To minimize the experiments, the experimental design was conducted by applying Design-Expert software based on the central composition method with 20 runs and 6 replicates of the central parts. The solvent extraction experiments were carried out at room temperature and far from flooding situations of the column.

6. Image Analysis Procedure

In the first step, the active section of the extraction column was filled by the aqueous phase and then the organic phase entering the column. Next, the required ranges for the operational parameters were selected. The mean drop sizes were obtained with the photographic methodology by applying a high-resolution digital camera (Nikon D5000). Droplet dimensions were processed with ImageJ software in terms of categorizing thresholding methods. In each run, 1000 droplets were analyzed by software for the certainty of the statistical importance of the drop size. The organic phase droplets typically were spherical; however, non-spherical shapes were also observed in the taken pictures. Thus, the following equation is presented for calculating the equivalent diameter of the ellipsoidal drops in which d_1 and d_2 represent the major and minor axes, respectively.

$$d_e = \sqrt[3]{d_1^1 d_2} \tag{28}$$

The average droplet size has then calculated as follows:

$$d_{32} = \frac{\Sigma_{i=1}^{n} n_i d_i^3}{\Sigma_{i=1}^{n} n_i d_i^2} \tag{29}$$

7. Dispersed Phase Holdup

At the end of each step, the free volume fraction of the dispersed phase was calculated with the shutdown approach. The inlet and outlet valves of the mass transfer device were rapidly closed while the steady-state situations were established. The continuous and dispersed phases were separated from each other, and then the holdup values were calculated by the following equation:

$$\varphi = \frac{\forall_d}{\forall_d + \forall_c} \tag{30}$$

In this work, the values of root mean square error (RMSE) and average absolute relative error (AARE) were employed to evaluate the presented models. These parameters of statistical analysis were calculated by the following equations:

$$\text{AARE} = \frac{1}{\text{NDP}} \sum_{i=1}^{NDP} \frac{|\text{Experimental data} - \text{Predicted data}|}{\text{Experimental data}} \tag{31}$$

$$\text{RMSE} = \sqrt{\frac{1}{\text{NDP}} \sum_{i=1}^{NDP} (\text{Experimental data} - \text{Predicted data})^2} \tag{32}$$

MATHEMATICAL MODELING

Several methods were developed for interpreting the mass transfer behavior in the horizontal and vertical columns. The axial dispersion method is suitable for investigating the mass transfer coefficients owing to the relative facility in column performance with the attainment of nearly precise results. Consequently, reactive mass transfer data along the mentioned extraction column wer determined by the axial dispersion approach. The movement of aqueous and organic phases in the perfect plug flow is the easier methodology to evaluate the mass transfer based on the ideal presumption in which the residence time of both fluids for the vanadium ions is identical in the column. The column structure and counter-currents of phases cause to flow pattern in all of the directions to invalidate this assumption. For the first time, the axial dispersion coefficients of dispersed and continuous phases were expressed by Danckwerts for amalgamation into one parameter based on the influencing parameters in order to eliminate this imperfection [43]. The equation set of this model under steady-state situations, over the differential elements with the active height of the column can be established as below [44]:

$$\frac{\partial}{\partial Z}\left(x - \frac{1}{P_c}\frac{\partial x}{\partial Z}\right) + N_{oc}(x - x^*) = 0 \tag{33}$$

$$\frac{\partial}{\partial Z}\left(y + \frac{1}{P_d}\frac{\partial y}{\partial Z}\right) - N_{oc}\frac{V_c}{V_d}(x - x^*) = 0 \tag{34}$$

Boundary conditions are:

$$Z = 0 \rightarrow \begin{cases} \left(\frac{U_c}{E_c}\right)(1 - X^0) = -\left.\frac{dX}{dZ}\right|_0 \\ \left.\frac{dY}{dZ}\right|_0 = 0 \rightarrow Y^0 = Y^{out} \end{cases} \tag{35}$$

$$Z = 1 \rightarrow \begin{cases} \left.\frac{dX}{dZ}\right|_1 = 0 \rightarrow X^1 = X^{out} \\ \left(\frac{U_d}{E_d}\right)(Y^1) = -\left.\frac{dX}{dZ}\right|_1 \end{cases} \tag{36}$$

The superficial velocities are constant at any range of agitation rate. In the above equations, N_{oc}, P_d, and P_c are defined as follows:

$$N_{oc} = \frac{K_{oc} a H}{V_c} \tag{37}$$

$$P_d = H\frac{V_d}{E_d} \tag{38}$$

$$P_c = H\frac{V_c}{E_c} \tag{39}$$

The axial mixing factor in the dispersed phase is lower than the axial mixing coefficient of the continuous phase. Thus, axial dispersion of the dispersed phase was considered insignificant, whereas the axial dispersion coefficient for the continuous phase was calculated by the following equation [45]:

$$\frac{E_c}{\overline{V}_c h_c} = -1.463 + 0.442\left(\frac{V_d}{V_c}\right) + \left[0.0012\left(\frac{ND_R}{V_c}\right) + \frac{23.15}{\left(\frac{ND_R}{V_c}\right) - 110.5}\right]\left(\frac{V_c D_R \rho_c}{\mu_c}\right)^{-0.27}\left(\frac{D_c}{D_R}\right)^{3.64}\left(\frac{D_c}{h_c}\right)^{1.34} e \tag{40}$$

The differential equations were numerically solved by Matlab software based on the central finite difference methodology. The overall mass transfer of the dispersed phase was obtained by applying the following relation, which M expresses the vanadium distribution ratio at the equilibrium conditions.

$$\frac{1}{mK_{od}} = \frac{1}{K_{oc}} \tag{41}$$

The interfacial area is also defined by the following equation:

$$a = \frac{6\varphi}{d_{32}} \tag{42}$$

RESULTS AND DISCUSSION

1. Batch Experiments

The extraction efficiency of vanadium from sulfate solution was studied by changing D_2EHPA concentration at various pH of the aqueous phase. The effect of extractant concentration and initial pH on the extraction rate is shown in Fig. 1(a). As can be observed, vanadium (V) extraction enhances by an increase in the D_2EHPA concentration from 0.05 to 0.3 M and afterward remains nearly fixed by further increment in the extractant concentration. In the constant extractant concentration, the impact of initial pH on the vanadium behavior indicates that the extraction rates increase by increasing the pH range from 1 to 2 and then reduce by further enhancement in this factor. The various predominant species for vanadium depend on the acidity of aqueous phase solution. The formation of VO_2^{2+} ions is created at a lower pH range than 2, which can be extracted by D_2EHPA and the reaction mechanism is written as follows:

$$VO_{2_{aq}}^{+} + (R_2HPO)_{org} \leftrightarrow VO_2(R_2PO_4)_{org} + H_{aq}^{+} \tag{43}$$

R signifies C_8H_{17} in the above equation. The synergistic effect of extractants improves the extraction efficiency, increasing the stability of complexes, removes emulsification. To investigate the synergism of solvent extraction, adding the TBP as a neutral extractant into the D_2EHPA system is studied on the solvent extraction process. Fig. 1(b) displays the extraction percentage and synergistic enhancement factor against TBP concentration, while the aqueous phase pH and the concentration of another extractant remain constant at 2 and 0.3 M, respectively. The extraction rate of vanadium increases sharply with raising the TBP concentration from 0.09 to 0.36 M, whereas the trend of plotted curve remains nearly constant. Therefore, the experimental results express that the synergistic effect of D_2EHPA and TBP is an appropriate choice for vanadium recovery in sulfate medium. The loaded organic phase contained 180 g/L of vanadium, which was stripped by different stripping agents. The stripping tests were conducted with different concentrations of stripping agents from 0.25 to 2 M at the equal ratio of the organic to aqueous phases. According to Fig. 2, acidic solutions have a negligible impact on the back extraction of vanadium from loaded organic phase in lower concentrations. For NH_4OH, the stripping rate of vanadium increases with enhancement in the stripping agent concentration up to 1 M; next, the effect of this parameter is insignificant due to increasing the viscosity. Eventually, the values of the aqueous pH, concentration of D_2EHPA, TBP, and NH_4OH were selected at 2, 0.3 M, 0.36 M, and 1 M, respectively, for subsequent experiments in the modified RDC column.

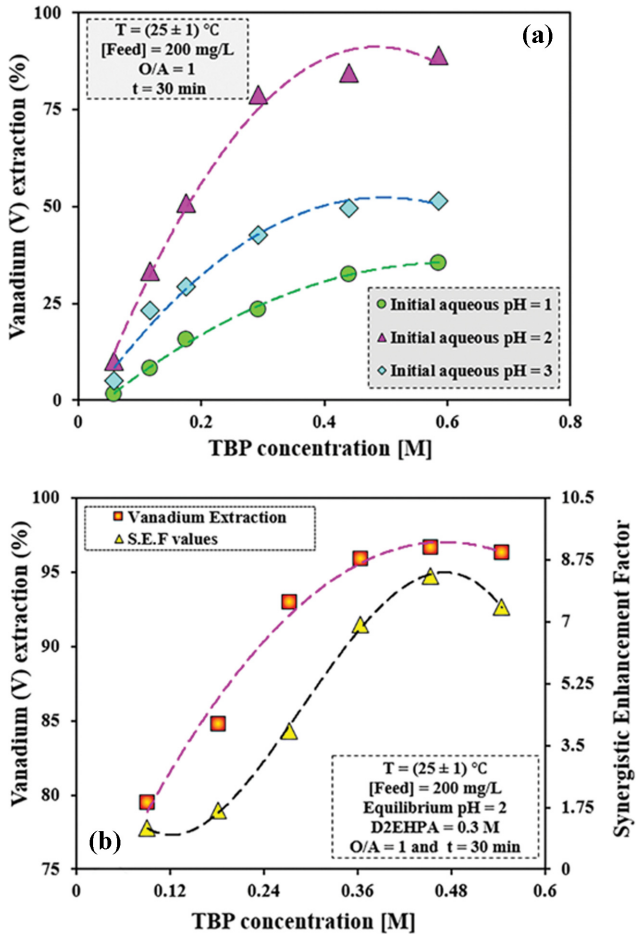

Fig. 1. Behavior of extraction rate against (a) aqueous phase pH and D_2EHPA concentration (b) synergism effect.

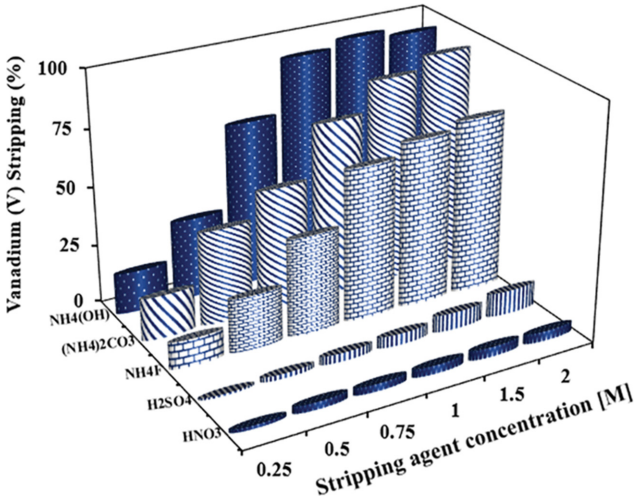

Fig. 2. Effect of different concentrations of stripping agents on the stripping efficiency (contact time=30 min and A/O=1).

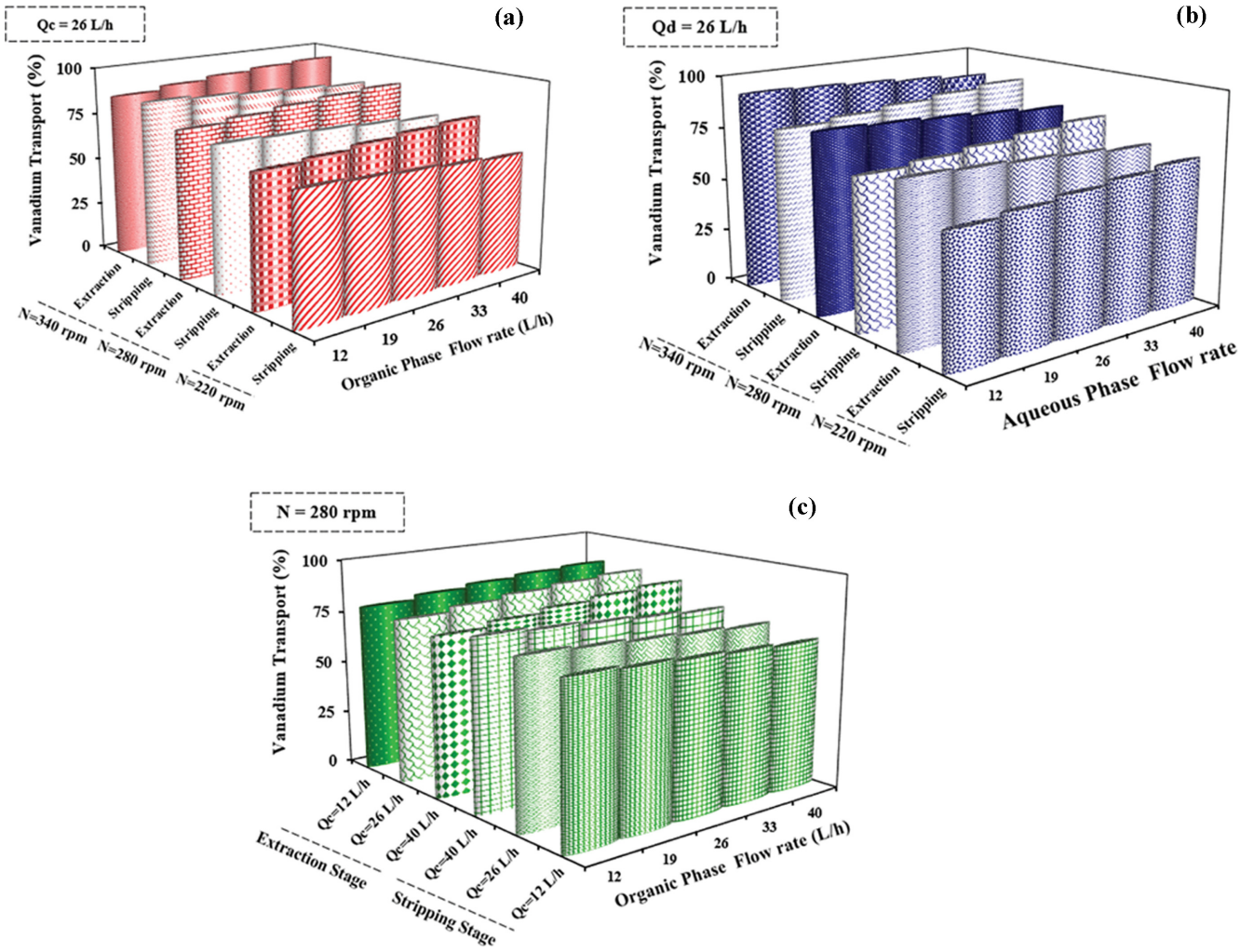

Fig. 3. Effect of operational parameters on the vanadium transport in extraction and stripping stages.

2. Continuous Experiments

By considering the central composition approach, the design of the experiments was performed that the operating ranges for agitation speed, organic phase flow rate, and aqueous phase flow rate.

2-1. Investigation of Vanadium Interactions

The vanadium interactions with changes in the operating variables, such as agitation speed and phase flow rates, were studied to optimize the maximum efficiency. The vanadium behavior between two phases is displayed with three-dimensional plots in the extraction and stripping stages. The solvent extraction results for both mass transfer directions are presented via the response surface method in Fig. 3. As shown in Fig. 3(a), faster equilibrium conditions and better reaction rate of vanadium occurred at high agitation speeds, which this phenomenon leads to improvement in the mass transfer coefficients by formatting the larger interfacial area. The extraction of vanadium was boosted by an enhancement in the flow rate of the organic phase. This observation is related to the increment of the amount of the D_2EHPA and TBP to extract the vanadium ions. In the stripping stage, the undesirable disturbances between the loaded organic phase and ammonium solution in more flow rates of the organic phase cause the reduction of vanadium stripping rate. The impact of the flow rate of the aqueous phase on the vanadium transport in order to investigate the extraction and stripping efficiencies is shown in Fig. 3(b). Compared with the turbulence of the aqueous phase, increasing the ammonium ions at higher aqueous phase velocity has more effect on the back extraction rate, which leads to an enhancement in the stripping percentage of vanadium. An increase in the turbulence phenomenon between the aqueous phase and the organic phase drops at a higher continuous phase flow rate reduces the vanadium transport into the organic phase along the mentioned column. Fig. 3(c) indicates the separation trend for vanadium species in two mass transfer directions in terms of velocities of aqueous and organic phases. The experimental findings show that the agitation speed has more effect on the distribution coefficients in comparison with the inlet phase velocities in the MRDC extraction column.

2-2. Investigation of Dispersed Phase Holdup

Knowledge of dispersed phase holdup is one of the most critical parameters for calculating the mass transfer kinetics in designing solvent extraction columns. This factor directly affects the interfacial area and slip velocity of droplets. The impact of the operational parameter on the holdup values in the extraction stage is

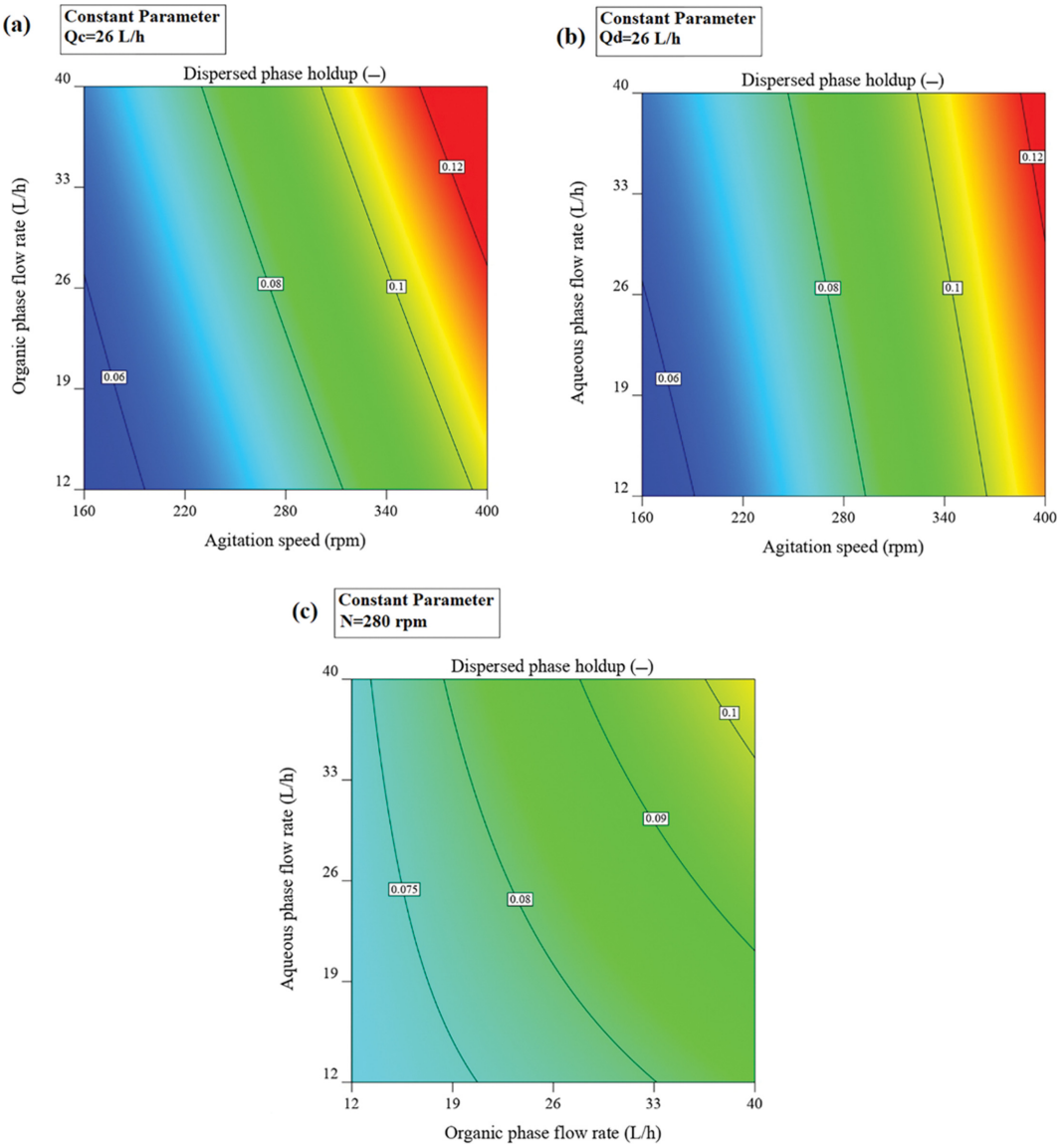

Fig. 4. Effect of operational parameters on the dispersed phase holdup for extraction stage.

demonstrated in Fig. 4. An increase in the shear forces at greater agitation speeds decreases the interconnection of droplets and increases the drops decomposition into smaller ones, which the dispersed phase holdup enhances along this column. The number of the organic phase droplets is enhanced by increasing the velocity of the organic phase into the column. Consequently, improvement of the flow rates of the dispersed phase leads to developing the values in the dispersed phase holdup. As can be seen, the continuous phase flow rate has a direct relation with the holdup values based on the increment in drag force of dispersed phase droplets with the continuous phase flow.

2-3. Modified Model for Dispersed Phase Holdup

Many researchers have presented various models for evaluating the dispersed phase holdup in agitated extraction columns. It is found that applying this factor is a convenient methodology to obtain the specific interfacial area and slip velocity of droplets. An experimental study on the molybdenum separation from tungsten was conducted by Shakib et al. in the PRDC column in which the following correlation is proposed to predict the holdup of dispersed phase based on the reactive and physical systems [46]:

$$\varphi = C\left(\frac{N^4 D_R^4 \rho_c}{g\sigma}\right)^{0.074}\left(1+\frac{V_c}{V_d}\right)^{0.079}\left(\frac{\mu_d}{\mu_c}\right)^{-0.218}\left(\frac{\rho_d V_d^2 D_c}{\sigma}\right)^{0.137} \quad (44)$$

The impact of reaction systems and mass transfer direction on the holdup of the dispersed phase is also shown by constant parameters. The present experimental results and the calculated values from Eq. (44) has been compared and the values for AARE and RMSE are 17.51% and 1.62%, respectively. The difference in the column geometries and particular systems leads to prediction deviation in the solvent extraction data. Therefore, a modified model is proposed by adding the geometric term to mentioned model to convert the statistical errors for validating the experimental results. After 30 iterations, model convergence was achieved by applying EViews software based on the Gauss-Newton algorithm and Mar-

Table 2. The values of the constant parameter, AARE, RMSE, and R^2 in the suggested model

Mass transfer conditions	C_1	AARE%	RMSE%	R^2
No reaction	0.296	8.767	1.110	0.908
Extraction stage (c→d)	0.308	7.219	0.738	0.957
Stripping stage (d→c)	0.262	9.719	0.838	0.947
All results		8.472	0.961	0.932

quardt steps, which is proposed as follows:

$$\varphi = C_1\left(\frac{N^2 D_c}{g}\right)^{0.338}\left(1+\frac{V_c}{V_d}\right)^{0.292}\left(\frac{\rho_d V_d^2 D_R}{\sigma}\right)^{0.24}\left(\frac{\mu_d}{\mu_c}\right)^{-0.176}\left(\frac{\rho_d}{\rho_c}\right)^{-0.642}\left(\frac{D_R}{h_c}\right)^{0.55} \quad (45)$$

The operating variables, physical properties, reactive or non-reactive systems, mass transfer direction, and geometric parameters have been considered in this modified model as a function of dimensionless groups. The values of the constant parameter, relative deviation error, root mean square error, and coefficient of determination are presented in Table 2. The suggested model performance is appropriate to combine the reaction systems and column geometry based on the reduced statistical errors. Eq. (45) is derived based on the experimental results of the present work and the data taken from published papers for different RDC columns, which the comparison of predicted results from this equation with the present results and previous experimental data is indicated in Fig. 5. According to the proximity of the experimental data to the bisector line, this figure clearly shows that the accuracy of the recommended model is acceptable to estimate the dispersed phase holdup with solvent extraction data and the experimental results by other investigators.

2-4. Uncertainty and Sensitivity Analysis

Sensitivity analysis characterizes the impact of uncertainty or model changes on the calculation of the results. The proposed model was evaluated by uncertainty analysis to interpret the confidence intervals of the input variables based on the statistical dispersion. The operational variables, geometric term, physical or chemical

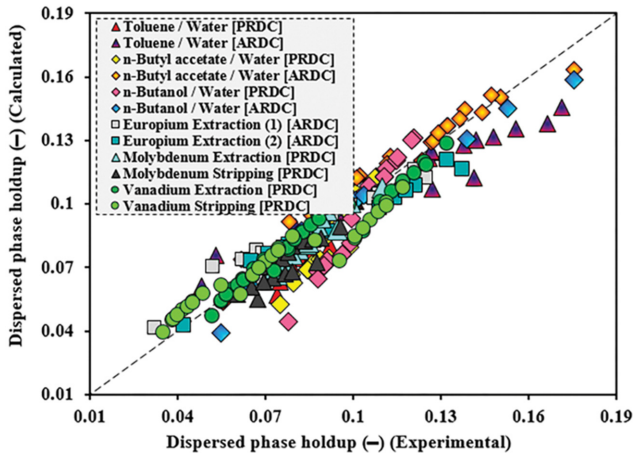

Fig. 5. Comparison between the calculated values from Eq. (45) and experimental results.

reaction situations, mass transfer direction, and physical properties of used systems were chosen for determining the sensitivity of dispersed phase holdup in the MRDC column under uncertainty analysis. The Monte-Carlo approach relies upon the central limit theory for providing the total appraisal of the uncertainty during the predictions constructed [47]. This technique simulates a total prediction owing to all the uncertainties in the input variables, irrespective of conducted observations and values of parameters. At first, input parameters are analyzed by applying a probability distribution function. 1000 Monte-Carlo iterations were repeatedly simulated by the new quantities randomly chosen to investigate the contribution of parametric study for uncertainty analysis on the response model determination using the Palisade/Risk software. A numerical simulation based on the triangular distribution function as a continuous probability distribution was carried out for input and output parameters. The results database was also developed from the numerous simulations using the MCA method for each of the parameters, for which a probability distribution histo-

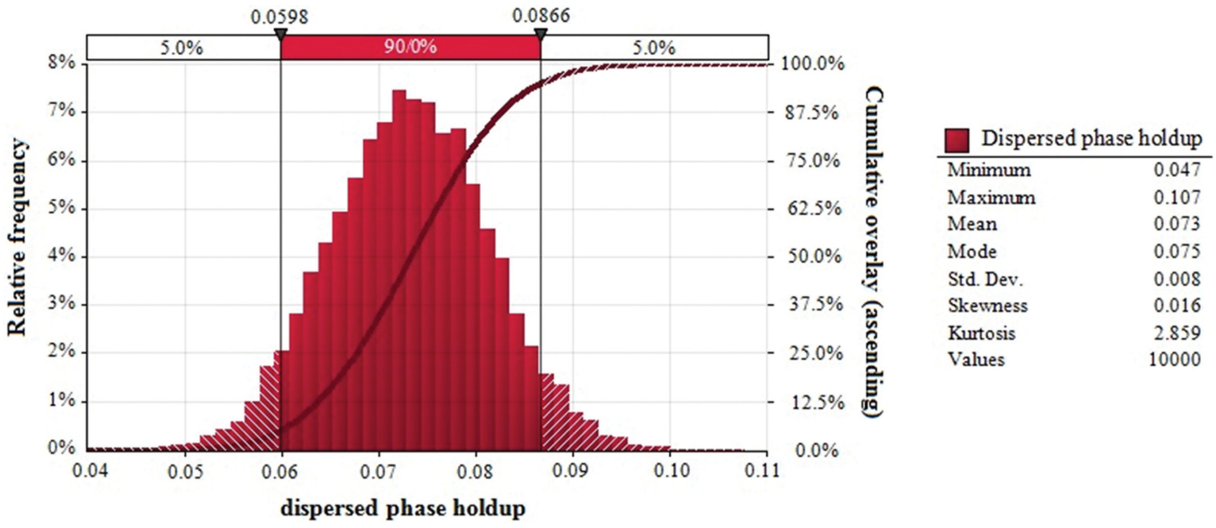

Fig. 6. Uncertainty analysis for dispersed phase holdup.

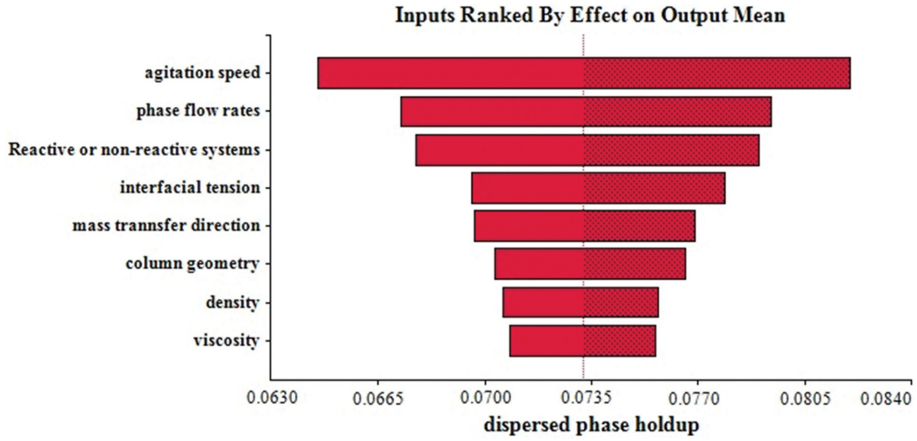

Fig. 7. Sensitivity analysis for dispersed phase holdup.

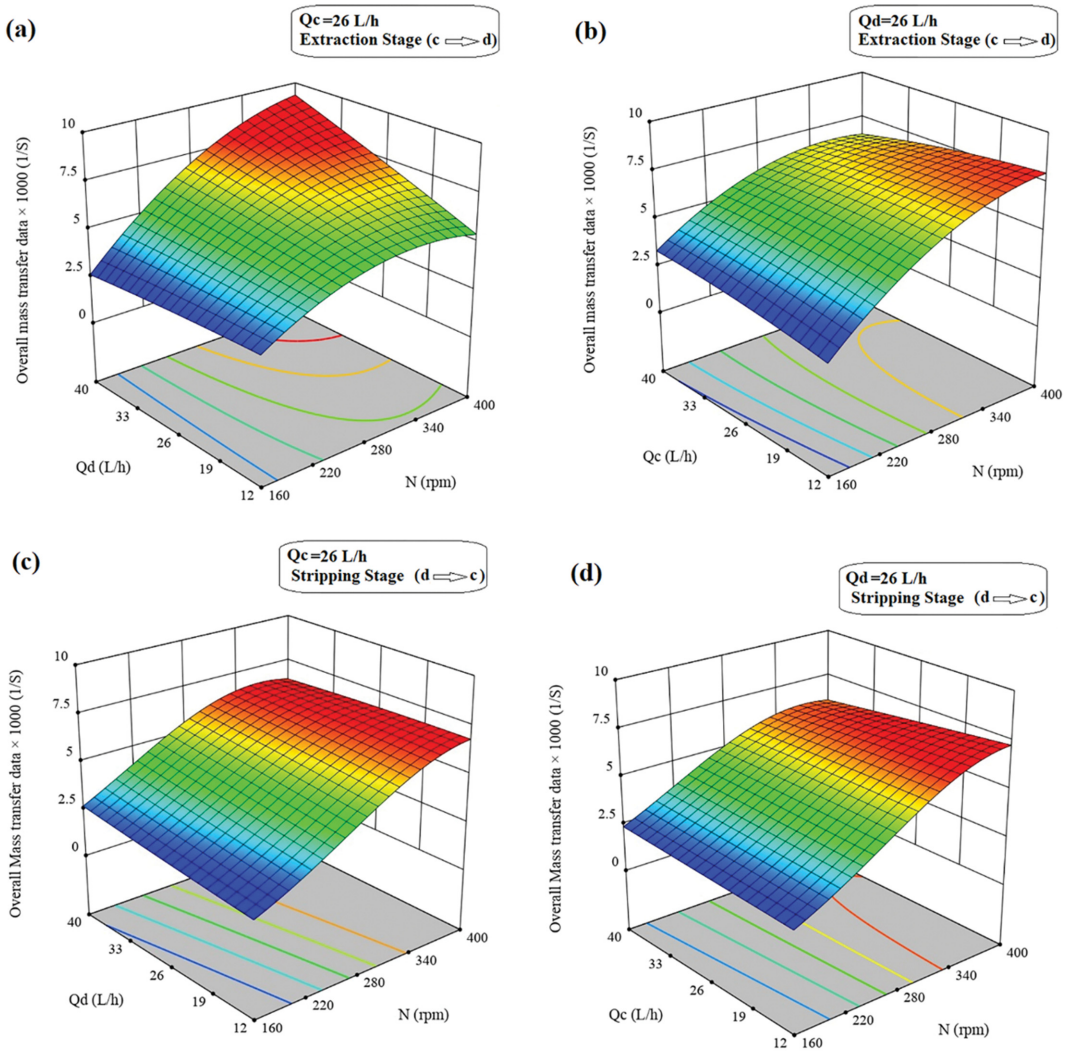

Fig. 8. Effect of operating parameters on the mass transfer rate for extraction and stripping stages.

gram to calculate the dispersed phase holdup based on the input distributions is shown in Fig. 6. Consequently, Fig. 7 shows the uncertainty predictions of the experimental data in order to evaluate the impact of eight input parameters on the sensitivity of holdup in terms of under the baseline value of 0.073. The reliability of results expresses that the agitation speed, phase flow rates, and reaction

situations have a great profound impact on the dispersed phase holdup. The influences of interfacial tension, mass transfer direction, and geometric parameters on this factor are considerable but weaker. Also, the holdup of the dispersed phase in the MRDC columns is slightly dependent on the viscosity and density parameters.

2-5. Investigation of Overall Mass Transfer Rate

The influence of operating parameters on the overall mass transfer data for extraction and stripping stages is shown in Fig. 8. It can be observed that the column performance significantly improves with increasing the agitation speed. A reduction in the internal circulation inside the solvent phase droplets in the higher rotor speed leads to reducing the mass transfer coefficients along the extraction column. The mass transfer data based on the axial dispersion methodology indicate that interfacial area has a great influence on the overall mass transfer rate in comparison with the mass transfer coefficients and, consequently, incremental behavior was observed on the column performance under reactive extraction systems. By considering the interactions of average droplet size and dispersed phase holdup in the back extraction stage, the reactive mass transfer coefficients due to internal circulations within drops are more than their values on the extraction stage. However, the impacts of mass transfer coefficients against the interfacial area are negligible on the overall mass transfer rate. As a result, the mentioned column performance in the extraction stage is more than the stripping stage under the chemical reaction systems. The variation of volumetric mass transfer coefficients along the modified RDC column with the perforated structure was studied for highlighting the influence of the organic phase rate on the reactive mass transfer rate. As can be observed from Fig. 8, the values of the volumetric overall mass transfer coefficients expand by an increase in the operational range in the solvent phase flow rate, because of the improvement in the overall mass transfer coefficients and interfacial area. It can be seen that the reactive mass transfer slightly reduces at a high aqueous phase flow rate. The overall mass transfer coefficients for vanadium extraction reduce owing to more turbulence between the aqueous phase and solvent phase droplets, although the effect of this function on the column performance is greater than the interfacial area. It was found that the effects of agitation speed and mass transfer direction on the reactive mass transfer rate were more pronounced than the phase flow rates for chemical reaction conditions in the MRDC column.

2-6. New Models for Reactive Mass Transfer

No equation for interpreting the overall mass transfer rate under the reactive extraction system is available for the RDC column with the perforated structure in the literature. A number of models to predict the column performance based on the dispersed phase were reviewed in order to create a comparison with the reactive mass transfer data. The average absolute relative error and root mean square error for the calculated quantities using mentioned models to the mass transfer results for vanadium solvent extraction at both directions are given in Table 3. As can be observed, none of the published models are capable of determining the reactive mass transfer in the MRDC extractor. The differences between the predicted values and experimental results are owing to the fact that the previous semi-empirical equations have been studied for mass transfer conditions without chemical reaction systems in other types of extraction columns. Hence, a new model development to calculate the volumetric overall mass transfer coefficients based on

Table 3. The values of AARE and RMSE in the predicted mass transfer rate with the published models

Equation	AARE%		RMSE	
	Extraction stage	Stripping stage	Extraction stage	Stripping stage
Gröber, Eq. (1)	18.301	16.886	0.385	0.436
Kronig and Brink, Eq. (2)	67.128	66.666	1.241	1.364
Handlos and Baron, Eq. (3)	42.194	39.46	0.806	0.863
Johnson and Hamielec, Eq. (4)	68.011	91.612	1.651	3.028
Boyadzhiev et al. Eq. (5)	86.194	80.100	1.529	1.654
Steiner, Eq. (6)	45.309	32.257	0.705	0.666
Hemmati et al. Eq. (7)	171.74	254.98	4.182	7.208
Asadollahzadeh et al. Eq. (8)	87.170	119.52	1.951	3.275
Bahmanyar et al. Eq. (9)	250.30	199.70	3.878	3.901
Torab-Mostaedi et al. Eq. (10)	152.375	259.21	2.745	5.530
Steiner et al. Eq. (11)	52.076	48.925	0.978	1.058
Rahbar-Kelishami et al. Eq. (12)	43.808	57.943	1.002	1.940
Shakib et al. Eq. (13)	18.821	16.982	0.534	0.444
Torab-mostaedi et al. Eq. (14)	38.425	55.160	1.041	1.716
Torkaman et al. Eq. (15)	144.08	241.36	3.332	4.725
Amanabadi et al. Eq. (16)	79.267	93.38	1.665	2.387
Hemmati et al. Eq. (17)	44.026	50.988	0.991	1.352
Torab-mostaedi et al. Eq. (18)	57.436	61.918	1.079	1.308
Torab-Mostaedi et al. Eq. (19)	53.210	40.058	0.924	0.862
Kumar and Hartland, Eq. (20)	80.705	76.923	1.408	1.559

Table 4. The values of the constant parameter and statistical analysis for the obtained model

Mass transfer direction	C_2	AARE%	RMSE	R-Square	D.W.S	Std. Dev.
Extraction stage (c→d)	5.31	4.868	0.163	0.932	0.759	0.463
Stripping stage (d→c)	5.54	3.987	0.169	0.922	0.658	0.427

the dispersed phase is one of the purposes of the current survey. Reactive mass transfer data are utilized in Eq. (4) for determining the enhancement factor. After calculating the experimental data of enhancement factor for reactive systems, the following model was derived by applying the least-squares methodology in EViews software:

$$R = C_2\left(\frac{\rho_C d_{32} V_S}{\mu_C}\right)^{-0.047}\left(\frac{\Delta\rho d_{32}^2 g}{\sigma}\right)^{0.153}(1-\varphi)^{3.068} \quad (46)$$

The effects of mass transfer direction for vanadium extraction were obtained by a constant parameter. The quantities for the constant parameter and the analysis of variance of the above equation are listed in Table 4. The obtained absolute relative errors indicate the high accuracy of the derived model for calculating the column performance under reactive extraction situations. In this survey, this correlation is proposed for extracting the vanadium ions from sulfate solution. It is expected that the mentioned model can be utilized for estimating the mass transfer performance of modified RDC columns at metallurgical processes, especially in the extraction of heavy metals.

CONCLUSION

Experimental and modeling studies were performed on the solvent extraction of vanadium by the synergistic effect of D_2EHPA and TBP by applying the response surface approach and Monte-Carlo simulation in the MRDC column. The experiments were investigated in this column using the central composition methodology to minimize and identify the impacts of input parameters. In the batch experiments, the values of 2, 0.3 M, 0.36 M, and 1 M were optimized for initial aqueous pH, the concentration of D_2EHPA, TBP, and NH_4OH, respectively. Next, the solvent extraction experiments were carried out in the mentioned column to investigate the hydrodynamic behavior and mass transfer characteristic. The dispersed phase holdup, extraction and stripping efficiencies, and reactive mass transfer rate were investigated via changes in the operating parameters. Numerical simulation on the uncertainty analysis of experimental data by the MCA method shows that the agitation speed, phase flow rates, and type of reaction systems have significant effects on the dispersed phase holdup in this column. A modified correlation to interpret the holdup values has been suggested based on the operating parameters, reaction conditions, physical properties, column geometry, and mass transfer direction by genetic algorithm optimization approach. Mass transfer rate based on the dispersed phase increases by an enhancement in the rotor speed and organic phase flow rate, but slightly decreases at a high flow rate of the aqueous phase. Compared with the aqueous and organic phase flow rates, the output results indicate that the agitation speed and extraction or stripping stages have strong effects on the column performance. In the current research, published works in different pulsed and agitated columns were reviewed to investigate the mass transfer coefficients. Disagreement in the predicted results with the present data was observed because these correlations were applied only to physical systems and particular geometries. Thus, a new equation for calculating the overall mass transfer rate based on the enhancement factor was introduced by considering the chemical resistance to mass transfer in the modified RDC column. This experimental and numerical study has provided noteworthy knowledge on the reactive mass transfer in this column that can be used to design solvent extraction columns in hydrometallurgical engineering.

NOMENCLATURE

AARE : average absolute relative error [-]
a : interfacial area [m^2/m^3]
B_n : nth coefficient in Eqs. (1)-(4) [-]
d_{32} : sauter mean diameter [m]
d_i : drop diameter [m]
d_e : equivalent diameter [m]
D_c : column diameter [m]
D_{eff} : effective diffusivity [m^2/s]
D_R : disc diameter [m]
D_S : stator ring diameter [m]
Eö : Eötvös number [-]
E : axial mixing coefficient [m^2/s]
E% : extraction efficiency [-]
e : fractional free cross-sectional area [-]
g : acceleration due to gravity [m/s^2]
h_c : compartment height [m]
K : overall mass transfer coefficient [m/s]
m : distribution ratio [-]
N : rotor speed [rps]
N_{ox} : number of 'true' transfer unit [-]
NDP : number of data points [-]
Pe : Peclet number [-]
R : enhancement factor for mass transfer [-]
RMSE : root mean square error [-]
Re : Reynolds number [-]
Sc : Schmidt number [-]
S% : stripping efficiency [-]
S.E.F : synergistic enhancement factor [-]
t : time [s]
V : superficial velocity [m/s]
V_t : terminal velocity [m/s]
V_S : slip velocity [m/s]
$\overline{V}_c$: continuous phase true velocity [m/s]
$\forall$: volume of the extraction region [m^3]

x : vanadium mass fraction in continuous phase [-]
x^* : equilibrium mass fraction [-]
y : vanadium mass fraction in dispersed phase [-]

Greek Letters

ρ_c : density of aqueous phase
ρ_d : density of solvent phase
μ_d : viscosity of solvent phase
μ_c : viscosity of aqueous phase
φ : dispersed phase holdup
σ : interfacial tension

REFERENCES

1. R. Moskalyk and A. Alfantazi, *Miner. Eng.*, **16**, 793 (2003).
2. M. Tuzen, T. G. Kazi, D. Citak and M. Soylak, *J. Anal. Atomic Spect.*, **28**, 1441 (2013).
3. H. T. Truong, T. H. Nguyen and M. S. Lee, *Hydrometallurgy*, **171**, 298 (2017).
4. L. Zeng and C. Y. Cheng, *Hydrometallurgy*, **101**, 141 (2010).
5. Q. Shi, Y. Zhang, J. Huang, T. Liu, H. Liu and L. Wang, *Sep. Purif. Technol.*, **181**, 1 (2017).
6. A. K. Nayak, N. Devi and K. Sarangi, *Trans. Indian Inst. Met.*, **74**, 3155 (2021).
7. X. B. Li, C. Wei, J. Wu, C. X. Li, M. T. Li, Z. G. Deng and H. S. Xu, *Trans. Nonferrous Met. Soc. China*, **22**, 461 (2012).
8. H. Liu, Y. M. Zhang, J. Huang, T. Liu and D. S. Luo, *Sep. Purif. Technol.*, **215**, 335 (2019).
9. Z. Zhu, K. Tulpatowicz, Y. Pranolo and C. Y. Cheng, *Hydrometallurgy*, **154**, 72 (2015).
10. M. R. Yaftian, M. I. G. S. Almeida, R. W. Cattrall and S. D. Kolev, *J. Mem. Sci.*, **545**, 57 (2018).
11. G. Hu, D. Chen, L. Wang, J. C. Liu, H. Zhao, Y. Liu, T. Qi, C. Zhang and P. Yu, *Sep. Purif. Technol.*, **125**, 59 (2014).
12. X. Li, C. Wei, Z. Deng, M. Li, C. Li and G. Fan, *Hydrometallurgy*, **105**, 359 (2011).
13. M. R. Tavakoli and D. B. Dreisinger, *Hydrometallurgy*, **141**, 17 (2014).
14. P. N. Remya and M. L. Reddy, *J. Chem. Eng. Biotechnol.*, **79**, 434 (2004).
15. M. Asadollahzadeh, A. Ghaemi, M. Torab-Mostaedi and S. Shahhosseini, *Chinese J. Chem. Eng.*, **24**, 989 (2016).
16. R. Ettouney and M. El-Rifai, *Chem. Eng. Res. Des.*, **89**, 2228 (2011).
17. M. Asadollahzadeh, R. Torkaman, M. Torab-Mostaedi and M. Saremi, *Inter. J. Heat Mass Trans.*, **188**, 122638 (2022).
18. M. Asadollahzadeh, A. Hemmati, M. Torab-Mostaedi, M. Shirvani, A. Ghaemi and Z. Mohsenzadeh, *Chinese J. Chem. Eng.*, **25**, 53 (2017).
19. T. Murugesan and I. Regupathi, *J. Chem. Eng. Japan*, **37**, 1293 (2004).
20. Z. Jia-Wen, Z. Shou-Hua, Z. Xiao-Kui, C. Xiao-Xiang, S. Yuan-Fu and A. Vogelpohl, *Chem. Eng. Technol.*, **14**, 167 (1991).
21. X. Chen, K. Li and Y. Su, *Ind. Eng. Chem. Res.*, **32**, 453 (1993).
22. N. V. Hendre, V. Venkatasubramani, R. A. Farakte and A. W. Patwardhan, *Ind. Eng. Chem. Res.*, **57**, 1630 (2018).
23. B. Kadam, J. Joshi and R. Patil, *Chem. Eng. Res. Des.*, **87**, 756 (2009).
24. N. V. Hendre, S. P. Hinge and A. W. Patwardhan, *Ind. Eng. Chem. Res.*, **60**, 5945 (2021).
25. A. Porto, L. Sarubbo, J. Lima-Filho, M. Aires-Barros, J. Cabral and E. Tambourgi, *Bioprocess Eng.*, **22**, 215 (2000).
26. J. S. Coimbra, F. Mojola and A. J. Meirelles, *J. Chem. Eng. Japan*, **31**, 277 (1998).
27. M. Carneiro-da-Cunha, M. Aires-Barros, E. Tambourgi and J. Cabral, *Biotechnol. Tech.*, **8**, 413 (1994).
28. A. Hemmati, A. Ghaemi and M. Asadollahzadeh, *Sep. Sci. Technol.*, **57**, 225 (2022).
29. B. Shakib, R. Torkaman, M. Torab-Mostaedi, M. Saremi and M. Asadollahzadeh, *Chem. Eng. Process*, **171**, 108762 (2022).
30. M. Asadollahzadeh, R. Torkaman and M. Torab-Mostaedi, *Chem. Eng. Process*, **169**, 108608 (2021).
31. R. Torkaman, M. R. A. Rovais, M. Heydari, M. Torab-Mostaedi and M. Asadollahzadeh, *Prog. Nucl. Energy*, **147**, 104217 (2022).
32. B. Shakib, R. Torkaman, M. Torab-Mostaedi and M. Asadollahzadeh, *Inter. J. Heat Mass Trans.*, **185**, 122337 (2022).
33. M. Asadollahzadeh, R. Torkaman, M. Torab-Mostaedi and M. Saremi, *Sci. Rep.*, **12**, 1609 (2022).
34. A. Hemmati, A. Ghaemi and M. Asadollahzadeh, *Sep. Sci. Technol.*, **56**, 2734 (2020).
35. B. Shakib, A. Ghaemi, A. Hemmati and M. Asadollahzadeh, *Prog. Nucl. Energy*, **141**, 103969 (2021).
36. H. Gröber and Z. Var, *Dtsch. Ing.*, **69**, 705 (1925).
37. R. Kronig and J. Brink, *Appl. Sci. Res.*, **2**, 142 (1951).
38. A. Handlos and T. Baron, *AIChE J.*, **3**, 127 (1957).
39. A. I. Johnson and A. Hamielec, *AIChE J.*, **6**, 145 (1960).
40. A. Kumar and S. Hartland, *Ind. Eng. Chem. Res.*, **35**, 2682 (1996).
41. C. Wilke and P. Chang, *AIChE J.*, **1**, 264 (1955).
42. M. Torab-Mostaedi, A. Ghaemi and M. Asadollahzadeh, *Chem. Eng. Res. Des.*, **89**, 2742 (2011).
43. P. V. Danckwerts, *Chem. Eng. Sci.*, **2**, 1 (1953).
44. H. Pratt and G. Stevens, *Science and practise of liquid-liquid extraction*, Clarendon Press, Oxford (1992).
45. B. Shakib, R. Torkaman, M. Torab-Mostaedi and M. Asadollahzadeh, *Inter. Commun. Heat Mass Trans.*, **118**, 104903 (2020).
46. B. Shakib, R. Torkaman, M. Torab-Mostaedi and M. Asadollahzadeh, *Chem. Pap.*, **74**, 4295 (2020).
47. I. Macdonald and P. Strachan, *Energy Build.*, **33**, 219 (2001).
48. L. Boyadzhiev, D. Elenkov and G. Kyuchukov, *Canadian J. Chem. Eng.*, **47**, 42 (1969).
49. L. Steiner, *Chem. Eng. Sci.*, **41**, 1979 (1986).
50. A. Hemmati, M. Torab-Mostaedi and M. Asadollahzadeh, *Chem. Eng. Res. Des.*, **93**, 747 (2015).
51. M. Asadollahzadeh, S. Shahhosseini, M. Torab-Mostaedi and A. Ghaemi, *Chem. Eng. Res. Des.*, **100**, 104 (2015).
52. H. Bahmanyar, L. Nazari and A. Sadr, *Chem. Eng. Process*, **47**, 57 (2008).
53. M. Torab-Mostaedi, A. Ghaemi and M. Asadollahzadeh, *Canadian J. Chem. Eng.*, **90**, 1570 (2012).
54. L. Steiner, A. Kumar and S. Hartland, *Canadian J. Chem. Eng.*, **66**, 241 (1988).
55. A. Rahbar, Z. Azizi, H. Bahmanyar and M. A. Moosavian, *Canadian J. Chem. Eng.*, **89**, 508 (2011).
56. B. Shakib, M. Torab-Mostaedi, M. Outokesh and M. Asadollahzadeh, *Heat Mass Trans.*, **56**, 1995 (2020).
57. M. Torab-Mostaedi, M. Asadollahzadeh and J. Safdari, *Chinese J.*

Chem. Eng., **25**, 288 (2017).
58. R. Torkaman, M. Torab-Mostaedi, J. Safdari, S. M. A. Moosavian and M. Asadollahzadeh, *Iranian J. Chem. Chem. Eng.*, **36**, 145 (2017).
59. M. Amanabadi, H. Bahmanyar, Z. Zarkeshan and M. A. Mousavian, *Chinese J. Chem. Eng.*, **17**, 366 (2009).
60. A. Hemmati, M. Shirvani, M. Torab-Mostaedi and A. Ghaemi, *Chem. Eng. Process*, **100**, 19 (2016).
61. M. Torab-Mostaedi, J. Safdari, M. Ghannadi-Maragheh and M. A. Moosavian, *J. Chem. Eng. Japan*, **42**, 78 (2009).
62. M. Torab-Mostaedi and J. Safdari, *Brazilian J. Chem. Eng.*, **26**, 685 (2009).